IEEE Access
Multidisciplinary ⋮ Rapid Review ⋮ Open Access Journal

Received 8 August 2022, accepted 6 September 2022, date of publication 8 September 2022, date of current version 19 September 2022.

Digital Object Identifier 10.1109/ACCESS.2022.3205319

RESEARCH ARTICLE

Channel Assignment Based on CSMA-Aware Interference Model With Overlapped Channels in Multiradio Multichannel Wireless Mesh Networks

YI TIAN[1,2], (Graduate Student Member, IEEE), AND TAKUYA YOSHIHIRO[3], (Member, IEEE)
[1]Graduate School of Systems Engineering, Wakayama University, Wakayama 6408510, Japan
[2]Department of Information Management, Shangluo University, Shangluo, Shaanxi 726000, China
[3]Faculty of Systems Engineering, Wakayama University, Wakayama 6408510, Japan

Corresponding author: Yi Tian (472575637@qq.com)

This work was supported by the Telecommunications Advancement Foundation.

ABSTRACT Multi-radio Multi-channel Wireless Mesh Networks (MRMC WMNs) implemented on IEEE 802.11 standards are widely used owing to their adaptability in practical network scenarios. The channel assignment problem in MRMC WMNs has been extensively studied. However, in most of the existing works, only orthogonal wireless channels are considered owing to the complexity of the channel assignment problem, which results in a low level of spatial utilization. This paper introduces partially overlapping channels into the CSMA-aware interference and shared link capacity models to fully exploit the spectrum resource and improve network capacity, utilizing both orthogonal channels and partially overlapping channels in IEEE 802.11 2.4 GHz bands. We formulate this problem as a mixed-integer linear program (MILP). We propose a traffic-demand-aware collision-free partially overlapping channel assignment (TAC-POCA), which uses all the available channels and achieves collision-free end-to-end flow transmissions to attain load balance. Simulation results show that TAC-POCA leads to better utilization of the spectrum resource and throughput improvement in both grid and random topology networks than in the case of using only orthogonal channels.

INDEX TERMS Partially overlapping channels, MRMC WMNs, channel assignment, collision-freedom, MILP.

I. INTRODUCTION

Wireless Mesh Networks (WMNs) are widely used in surveillance, building automation, remote health care delivery, smart grids, and so on, owing to their convenience in ease of implementation, low cost, and immense adaptability in practical scenarios [1], [2]. Especially, area coverage via Wi-Fi with stationary or drone infrastructure is a promising usage of WMNs. With WMNs, data collection and distribution without wired infrastructure is enabled, and various IoT applications will work on it. Here, with the growing demand for multimedia applications, WMNs are expected to support heterogeneous traffic types (e.g., voice, video, and data traffic) with various quality-of-service (QoS) requirements [3], [4]. Interference from adjacent parallel transmissions decreases capacity, which becomes a major problem in WMNs. An efficient way to minimize this problem is to use multiple interfaces configured on distinct channels per node, which is called multi-radio multi-channel (MRMC) technology [5], [6], [7], [8], [9], [10], [11]. In MRMC WMNs, channel assignment becomes a critical issue, which requires the assignment of each radio of each node to an appropriate channel to maximize the network performance.

The IEEE 802.11 standards are currently the most commonly used radio protocol for MRMC WMNs, and MRMC WMNs based on IEEE 802.11 2.4 GHz standards can utilize 13 distinct channels. However, these channels partially overlap rather than entirely orthogonal, and only three out of the 13 can be chosen as orthogonal channels (OCs). Typically, we assign three OCs for WMNs, which results in a low level of spatial utilization. It is difficult to support the rapid increase in IEEE 802.11 devices and wireless traffic

The associate editor coordinating the review of this manuscript and approving it for publication was Jiankang Zhang.

demands. Since the claim that partially overlapped channels can markedly improve frequency utilization has been posed by Mishra [12], [13], much effort has been devoted to designing efficient channel assignment schemes using partially overlapped channels (POCs) [14]. The use of POCs in channel assignment in wireless networks has received some attention.

As the interference among POCs affects communications between nodes, channel assignment aims to eliminate the interference in the network. Generally, channel assignment can be formulated either as an independent problem that takes into consider action interference among links [15], [16], [17], [18], [19], [20], [21] or as joint problems combined with other constraints. Routing would be one of the most effective ways to minimize collisions among links and improve the performance of networks because routing and channel assignment are highly dependent on each other. Channel assignment aims to reduce collisions, whereas routing also contributes to reducing collisions by removing potential interference among links, i.e., by avoiding a portion of links used as routing paths so that they do not cause interference. The combination of channel assignment and routing is effective because it can achieve collision-free scheduling with only three orthogonal channels by using a CSMA-aware interference model [22]. Development of joint channel assignment and routing schemes using OCs has been in progress for decades. However, the current literature has not applied POCs to joint channel assignment and routing schemes. The potential of channel assignment and routing combination under POCs in MRMC WMNs has not been sufficiently explored. In [24], [25], [26], and [27], the authors considered routing as a factor combined with channel assignment using POCs. Still, they all assumed that routing paths are predetermined, which lacks flexibility in traffic engineering. Optimal routes combined with channel assignment should be explored in the optimization scheme.

In [27], we proposed a combination of channel assignment and routing scheme traffic-demand-aware collision-free channel assignment (TACCA), which achieved collision-free transmission in 802.11-based MRMC WMNs. However, TACCA deals with channel assignment with OCs, resulting in a low level of spatial utilization. On the other hand, due to the difference in interference estimation between OCs and POCs, TACCA does not work when using POCs. Therefore, this paper proposes a new traffic-demand-aware collision-free partially overlapping channel assignment (TAC-POCA) scheme, introducing POCs into the CSMA-aware interference and the CSMA-aware shared capacity models TACCA to achieve collision-free transmission while considering traffic engineering. Note that the base channel assignment problem is NP-hard [22]. As a first and straightforward step, we mathematically formulate the situation as a mixed-integer linear optimization problem (MILP). By exploiting the excellent property of the spatial reuse of POC in combination with route optimization, we achieve a higher number of simultaneous transmissions than when using only OCs. We make the following contributions:

(1) We introduce POCs into the collision-free channel assignment scheme TACCA [27], which is based on the CSMA-aware interference model and the shared link capacity model, and design a reasonable channel assignment scheme to ensure the effectiveness of POCs.

(2) We jointly solve the channel assignment and routing problems using POCs, i.e., channel assignment and routing are treated simultaneously. We show that POCs are significantly effective in improving spatial reuse in WMNs.

Our new scheme significantly improves channel reuse and efficiently improves the network capacity. Without modifying the IEEE 802.11 protocol, we employ all channels in MRMC WMNs, and partially overlapped channels collaboratively work without collision. To the best of our knowledge, our scheme is the first joint channel assignment and routing scheme using POCs that achieve collision-free transmission.

This paper is the extended version of the preliminary paper [28] for which we not only complete the full description, including related work to improve the clarity in detail but also extend the problem and the model to consider the protocol model thoroughly and significantly expand the evaluation part to clarify the performance and contribution of our method.

To avoid ambiguity, let us note that the term ''collision freedom'' represents the zero-collision schedule (i.e., the channel assignment and routing) just under the rational interference model proposed in this paper. In this paper, we introduce an interference model based on the behavior of physical radio and the CSMA MAC protocol, and we obtain a zero-collision schedule through our MILP formulation. In theory, this schedule may not be precisely collision-free in the natural environment due to the gap between our model and reality.

The rest of this paper is organized as follows. We present related works in Sec. II. We describe the system model, interference model, shared link capacity model, and some assumptions in Sec. III. We formulate the problem in Sec. IV. Performance evaluations are given in Sec.V. Conclusions are given in Sec. VI.

II. RELATED WORK

For channel assignment, most existing research studies are confined to transmission to OCs and focused on mitigating co-channel interference by combining other aspects such as routing and QoS [29], [30], [31], [32], [33], [34], [35], [36], [37], [38], [39], [40], [41]. There are joint routing and link scheduling [29], [30], [31], [32], [33], [34], joint power control [35], [36], [37], joint QoS multicast routing [38], [39], etc. Among them, the joint routing approach may be one of the most promising ones for reducing collisions because routing directly controls the interference patterns. However, since a certain bandwidth should separate two adjacent orthogonal channels, orthogonal separation wastes spectrum resources. To enhance spectral utilization, the concept of POCs was

introduced. Mishra [12], [13] put forward the pioneering idea of using POCs. They showed that POC utilization could improve spectrum utilization and throughput by designing a practical interference model using POCs and demonstrating its application to channel assignment. After that, researchers successively carried out further investigations of the model. As mentioned earlier, routing is the most effective way to reduce collisions among links and improve the performance of networks. Two approaches are proposed for the surveyed channel assignment. In one method, channel assignment is viewed as a lower-layer mechanism and does not consider the traffic load. In contrast, routing is viewed as an upper-layer mechanism and is fully responsible for distributing the traffic load, i.e., routing is independent of channel assignment [15], [16], [17], [18], [19], [20], [21]. In the other approach, channel assignment and routing are mutually dependent, so they are combined to obtain optimal network performance. This study focuses on this combined channel assignment and routing with POCs to achieve collision-free transmission.

The routing configuration can effectively reduce interference among links because it can ''inactivate'' a portion of links by making no traffic use them, which removes potential interference to be considered in channel assignment. However, only a few studies on channel assignment using POCs considered the routing factor. Yang *et al.* [23] designed a POC assignment scheme with effective interference avoidance and load balancing for WMNs, but they assumed that the AODV routing protocol predetermines routing paths. Wang *et al.* [24] explored ways to exploit POCs to perform end-to-end channel assignment to achieve effective end-to-end flow transmissions and the proposed end-to-end load-aware partial channel assignment (ELIA-POCA) for MRMC WMNs. They also assumed that routing paths are pre-determined by the shortest routes. Liu *et al.* [25] proposed two load-aware channel assignment schemes, channel assignment exploiting partially overlapping channels (CAEPO) and load-aware CAEPO-G, to use the POCs for wireless mesh networks under the IEEE 802.11 standards. However, they used bandwidth-aware AODV to determine the routing paths, which are based on the shortest routes, and thus the performance in collision avoidance is limited.

Mohsenian-Rad *et al.* [26] proposed a joint channel assignment, interface assignment, and a scheduling algorithm for MRMC WMNs when all OCs and POCs are being used. The problem with this combination is formulated as a linear mixed-integer program with a few integer variables. Their method adopts an SINR-based interference model and considers pairwise interference between links. Simulation results show a significant performance improvement in achieving high network capacity and a low level of bottleneck link utilization when all the POCs within the IEEE 802.11 2.4 GHz frequency band are used. Although this work is somewhat similar to ours, there are three drawbacks. First, Mohsenian-Rad *et al.* also assumed that the routing paths are pre-determined. Second, although they used an SINR-based interference model, their model simply considers the pairwise effect between two links and does not consider the effects among multiple links, which is a partial consideration of the SINR model. Third, they do not consider the hidden-terminal effects; they assume that nearby links assigned with the same channel can share their capacity even if they are in a hidden-terminal relationship. As mentioned above, currently, no scheme simultaneously optimizes channel assignment and routing in the context of POC studies. We show the comparison of the above POC-based channel assignment methods in Table 1.

On the other hand, regarding OCs, several advanced joint channel assignment and routing schemes have been proposed. Some proposed joint solutions with other aspects such as routing, link scheduling, power control, and QoS. In addition, interference models used in the channel assignment have also been primarily developed. The most basic interference model is called the protocol model, in which the communication range and the interference range are defined as a circle, respectively [42]. Jia *et al.* [37] used the SINR model in a joint power control and channel assignment formulation. Chaudhry *et al.* used the SINR model with a shadowing effect [32] in a joint routing and channel assignment formulation, and proposed a heuristic algorithm that considers the cumulative nature of SINR interference model [33]. They further introduced a beam-forming effect in their formulation [34]. However, the number of channels required is not reduced enough, and 8-10 OCs are still needed for a collision-free channel assignment.

To reduce the number of required channels, we proposed a joint channel assignment and routing scheme called TACCA, which achieves collision freedom with 3-5 OCs in IEEE 802.11 2.4 GHz based MRMC WMNs by incorporating the CSMA-aware interference model [27]. In addition, to provide good load-balancing performance, TACCA minimizes the network-wide utility in a given traffic demand matrix. However, TACCA deals with channel assignment under OCs, resulting in low spatial utilization. Owing to the difference in interference estimation between OCs and POCs, POCs are not directly applicable to TACCA in WMNs. Therefore, this paper proposes a new scheme, TAC-POCA, that introduces POCs into the CSMA-aware interference model and the CSMA-aware shared capacity model to achieve collision-free transmission while considering traffic engineering. This is the first study incorporating the CSMA-aware interference model into POC-based channel assignment.

III. DEFINITION

In this section, we first introduce our network model and assumptions. After that, basic interference models among POCs are defined. Then, we extend the CSMA-aware interference model and shared link capacity model by introducing POCs, which specify our TAC-POCA scheme's key characteristics.

A. NETWORK MODEL AND ASSUMPTIONS

We model an MRMC WMN as nodes V connected by directed links E. Then, digraph $G = (V, E)$ represents the

TABLE 1. Comparison of POCs assignment techniques based on the combined routing.

Ref.	Interference Model	Assumed Traffic Model	Routing Consideration	Hidden Terminal Considered	Methods
TAC-POCA (Proposed)	Protocol model	End-to-end flows	Jointly solved in channel assignment	Yes	MILP
LBIA-POCA [20]	Protocol model	End-to-end flows	Predetermined	No	Heuristic (Centeralized)
ELIA-POCA [21]	Protocol model	No traffic model assumed	No	No	Heuristic (Centeralized)
CAEPO, CAEPO-G[22]	Protocol model	End-to-end flows	AODV-based	No	Heuristic (Distributed)
Mohsenian-Rad et al.[23]	SINR-based model (pairwise)	End-to-end flows	Predetermined	No	MILP

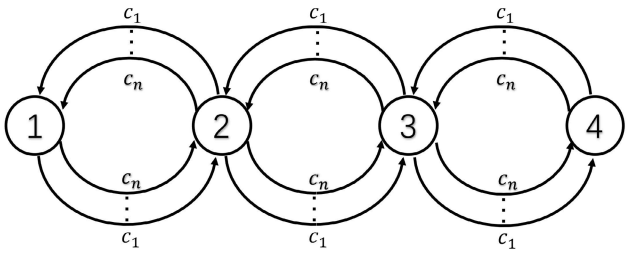

FIGURE 1. Network model.

network. We assume that each node in V is equipped with N_v classic NICs built on IEEE 802.11 technology, and each NIC operates on a distinct frequency channel. A link $l \in E$ that goes from node u to node v using channel $c \in C$ is written as $l = (u, v, c)$, where C is a set of channels. Then, there are potential $2|C|$ available links for communications between each pair of neighboring nodes u and v in V. Fig.1 illustrates the model of our network G, where $c_1 \ldots c_n$ represents the channel of the n $(= |C|)$ potential links from a sender node to a receiver.

We are given a traffic demand matrix D, which represents the amount of traffic demand from node s to d for each pair $(s, d) \in V \times V$. We write $D(s, d)$ to denote the amount of traffic demand from s to d. For each non-zero demand $D(s, d)$, we set a path for the traffic to move forward. Then, with each pair (s, d) and each link l, we associate a variable $P_l^{(s,d)} \in \{0, 1\}$ that indicates whether the traffic flow for demand (s, d) goes through link l or not, i.e., $P_l^{(s,d)} = 1$ when the routing path from s to d includes the link l, and $P_l^{(s,d)} = 0$ otherwise.

Neighboring nodes must be assigned to the same channel to communicate with each other. Then, if a link $l = (u, v, c)$ is used to transmit frames, the channel c must be assigned to one of the NICs of both u and v. We call the link used as a path of some flow the *active link*. To represent this, a variable $A_l \in \{0, 1\}$ is defined, where $A_l = 1$ indicates that link l is active and $A_l = 0$ inactive. On the other hand, we define a variable $R_v^c \in \{0, 1\}$, which indicates whether an NIC on node v is assigned with the frequency channel c or not, i.e., $R_v^c = 1$ if there is an NIC on node v assigned with the frequency channel c, and $R_v^c = 0$ otherwise. Naturally, if $A_{(u,v,c)} = 1$, then $R_u^c = R_v^c = 1$.

In this study, we minimize the maximum link utilization to achieve a good load balancing in the network. We assume that all links communicate at the same speed and have the same capacity defined as Θ. Then, the link utilization is the ratio of traffic amount to the link capacity Θ, i.e., the utilization of link $l \in E$ is expressed as $\sum_{(s,d)\in V\times V} D(s, d)P_l^{(s,d)}/\Theta$. Thus, we define the variable U_{max} where $0 \leq U_{max} \leq 1$, which represents the maximum link utilization among all links.

We sometimes use the term (u, v, c) in place of link l, where u and v are the terminal nodes of link l, and c is the assigned channel with link l. We provide additional definitions to introduce the collision-free and capacity constraint in the following sections. Problem formulation will be given in Sec. IV.

B. INTERFERENCE AMONG POCs

On the IEEE 802.11 2.4 GHz band, there are 13 available channels, each of which has a spread of about 22 MHz, and the center frequencies of channels are 5 MHz apart, as shown in Fig. 2. Therefore, any two channels separated over five channels are called OCs, e.g., channels 1, 6, and 11 are OCs, among which signals do not overlap. Otherwise, they are POCs whose signals overlap; e.g., channels 1 and 3 are POCs. Hoque *et al.* [18] classified the interference of IEEE 802.11-based MRMC WMNs into three types: (i) When two in-range transmitters operate on the same channel, they interfere with each other, and such interference is called co-channel interference (CCI). (ii) When two transmitters operate on relatively close channels that partially overlap, they cause a lesser degree of interference, referred to as adjacent channel interference (ACI). (iii) Transmissions on a NIC at a node interfere with those of another NIC at the same node if those two nodes are assigned with the same or non-orthogonal channels, which is defined as self-interference (SI). These three types of interference have to be eliminated to achieve collision-free transmission. It is known that an interference model is utilized for estimating the interference level among nodes. Therefore, designing an accurate interference model is essential to achieving collision-free transmission.

In this paper, interference is modeled based on a simple disk model (called the protocol model) [42], i.e., the *interference range* $(1 + \Delta)R$ is defined, where R indicates the communication range and $\Delta > 0$ is a constant. Then nodes

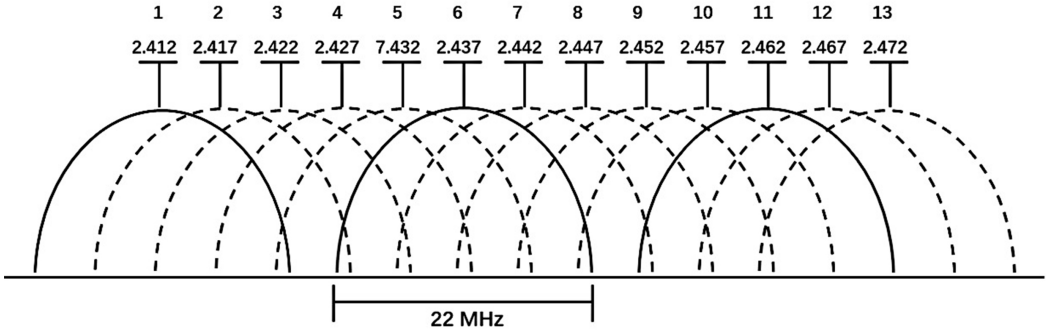

FIGURE 2. IEEE 802.11 2.4 GHz ISM band.

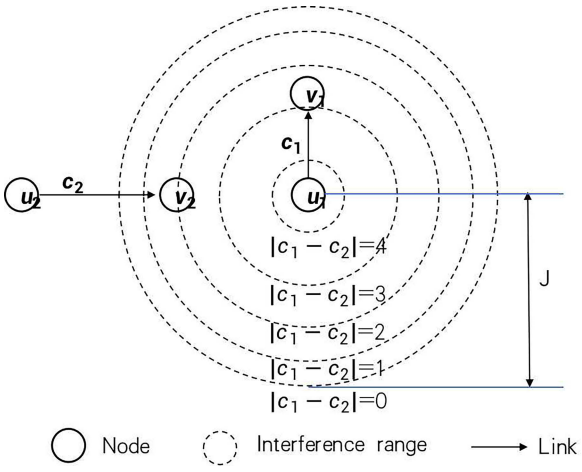

FIGURE 3. Interference ranges depending on the channel distance.

within the range $(1 + \Delta)R$ of a transmitter fail to receive any frame. This disk model is defined for CCI, and we extend it for POCs.

In Fig.3, in which two links (u_1, v_1, c_1) and (u_2, v_2, c_2) are located close to each other. If $c_1 = c_2$, then it is a CCI case; transmission on (u_1, v_1, c_1) collides with (u_2, v_2, c_2) and v_2 fails to receive frames because the distance between u_1 and v_2 is smaller than J, where $J = (1 + \Delta)R$. If the separation between c_1 and c_2 is 1, i.e., $|c_1 - c_2| = 1$, then it is an ACI case, and the interference range becomes slightly smaller than J. However, since v_2 is still within the interference range, v_2 still fails to receive frames. Similarly, as the separation between c_1 and c_2 becomes smaller, the interference range decreases accordingly, and v_2 can receive frames when the channel separation is 3. Finally, when the channel separation is larger than 4, the interference range is 0, and even SI does not happen.

To express the reduction in the interference range along with the level of channel separation, the range reduction ratio $I_{rrr}(c_1, c_2)$ is introduced, which takes the range [0,1] that indicates the reduction ratio of the interference range, i.e., $JI_{rrr}(c_1, c_2)$ is the interference range under two channels c_1 and c_2. When a node receives signals with the channel c_2, the interference ranges from other nodes depending on the transmitting channel c_1. Specifically, the interference

TABLE 2. Reduce interference range ratios.

Channel distance	0	1	2	3	4	≥ 5
$I_{rrr}(c,c_2)$	1	0.8667	0.6928	0.4739	0.1882	0

range decreases as the distance in frequency between c_1 and c_2 increases, and the range is zero (i.e., no interference) when the channel distance is more significant than 4. This interference model is introduced in [16], and similar models are commonly used in many studies. The values of $I_{rrr}(c_1, c_2)$ used in [16] are shown in Table 2, and in this paper, we also use these values.

C. CSMA-AWARE INTERFERENCE MODEL WITH POCs

The CSMA-aware interference model was proposed in [25], which significantly reduces collisions among frames in CSMA-based WMNs by considering the behavior of CSMA. However, it assumes to use OCs, and its performance is limited. This section introduces POCs into the CSMA-aware interference model to further improve the spatial reuse in WMNs.

Recall that the interference distance depends on both physical and channel separation distances, as described in the previous section. In our new CSMA-aware interference model, we simply apply this considering the property of CSMA. Specifically, we regard J as the *interference range* of the CCI case. Using the definition of the disk model, we also regard R as the *communication range* of the CCI case, within which two nodes can exchange frames with each other, and as the *carrier-sense range* of the CCI case, within which a node senses the other node's transmission in CSMA. As for the *carrier-sense range*, we apply a special treatment that the *carrier-sense range* is assumed to be far smaller than the *interference range* in the ACI case. This is our heuristic approach considering the real difference between the *carrier-sense range* and the *interference range*; when the signal received is weak, the interference is affected markedly by the nature of the SINR-based reception. Because we designed our model based on the disk model and the reduced interference range ratio $I_{rrr}(c_1, c_2)$ introduced from [16] is designed based on the interference effect, this heuristic approach is practical and makes capacity sharing more efficient.

Based on these assumptions, we now introduce three cases in which frames collide in our CSMA-aware interference model with POCs. Let $d(u, v)$ be the Euclidean distance between nodes u and v. Also, let $l_1 = (u_1, v_1, c_1)$ and $l_2 = (u_2, v_2, c_2)$ be a pair of two directed links in E, i.e., both $d(u_1, v_1) < R$ and $d(u_2, v_2) < R$ hold. Then, transmission on l_1 prevents communication on l_2 owing to collision if either of the following cases is met:

Case 1: Data frames collided with Data frames.

(1) $d(u_1, v_2) \leq JI_{rrr}(c_1, c_2)$,
(2) $d(u_1, u_2) > RI_{rrr}(c_1, c_2)$.

Case 2: Ack frames collided with Data frames.

(1) $d(v_1, v_2) \leq JI_{rrr}(c_1, c_2)$,
(2) $d(u_1, u_2) > JI_{rrr}(c_1, c_2)$,
(3) $d(u_1, v_2) > JI_{rrr}(c_1, c_2)$.

Case 3: Data frames collided with Ack frames.

(1) $c_1 \neq c_2 \wedge u_1 \neq u_2$,
(2) $d(u_1, u_2) \leq JI_{rrr}(c_1, c_2)$.

Case 1 provides the conditions for the transmission of Data frames on l_1 interferes with the reception of Data frames on l_2. See Fig. 4(a). Node v_2 is within the *interference range* $JI_{rrr}(c_1, c_2)$ of node u_1, but nodes u_1 and u_2 are not within the *carrier-sense range* $RI_{rrr}(c_1, c_2)$ which results in collision of Data frames when two Data frames are transmitted simultaneously on both l_1 and l_2. Note that nodes v_1 and v_2 may be the same node.

In Case 2 shown in Fig. 4(b), the transmission of Ack frames on l_1 interferes with the reception of Data frames on l_2. In this case, the reception nodes v_1 and v_2 are located within the *interference range* $JI_{rrr}(c_1, c_2)$, whereas the distances between u_1 and u_2, and between u_1, and v_2 are both larger than the *interference range* $JI_{rrr}(c_1, c_2)$, respectively. Then, u_1 and u_2 may transmit Data frames simultaneously, and Ack frames transmitted by v_1 interfere with Data frame reception of v_2.

In Case 3 shown in Fig. 4(c), Data frames on l_1 interfere with the reception of Ack frames on l_2. This occurs only in the case of ACI (i.e., $c_1 \neq c_2$), and we assume $u_1 \neq u_2$ to exclude self-interference (SI). Here, u_1 and u_2 are within the *interference range* $JI_{rrr}(c_1, c_2)$, but we assume that they cannot sense carriers of the other according to the special treatment for POCs stated in this section. In this case, both u_1 and u_2 transmit Data frames, and the returned Ack frames are interfered by the Data frames.

Note that the fourth case where two Ack frames collide is ignored because of its low probability of occurring. Even if this case is included in our channel assignment results, its effect on communication performance is sufficiently small.

According to the above definition of interference, we introduce a set of interference link pairs S_{ILP} that should be excluded from the solution of our channel assignment problem. Note that the interference is asymmetric, i.e., even if link l_1 prevents communication on l_2, l_2 may not prevent communication on l_1. Thus, we write an interference link pair under the above definition of three cases as $l_1 \rightarrow l_2$, and

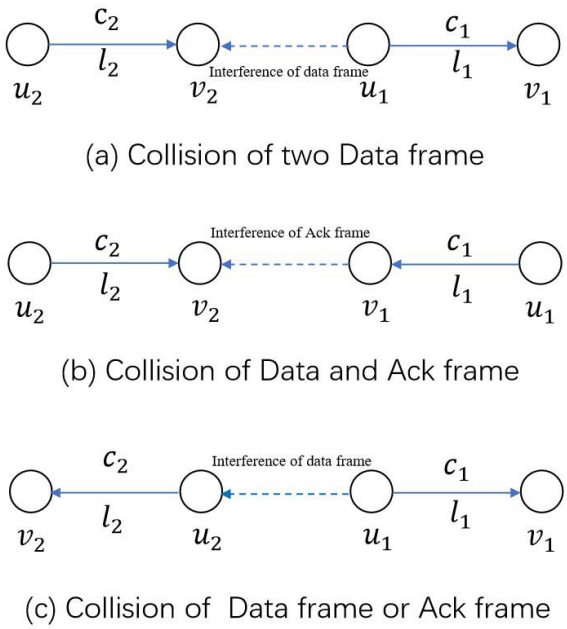

FIGURE 4. Interference model.

the set of interference link pairs in the network is defined as follows.

$$S_{ILP} = \{(l_1, l_2) | l_1, l_2 \in E, l_1 \rightarrow l_2\} \quad (1)$$

S_{ILP} is computed from the given network topology, and used in the MILP formulation of our joint channel assignment and routing problem.

D. SHARED LINK CAPACITY MODEL WITH POCs

The above CSMA-aware interference model enables us to prevent collisions that occur under the system of CSMA. On the other hand, CSMA's carrier sensing behavior also prevents collisions in CCI and SI cases. Combining those two, all collisions are eliminated in our scheme TAC-POCA.

However, we must note that CSMA's collision prevention mechanism based on carrier sensing enables a set of links to share the common communication resources. To balance the load within limited network resources, the total amount of traffic load on all the shared capacity links should not exceed the capacity Θ. In wireless networks, a channel as a resource is shared by nodes within the *carrier-sense range*; thus, the links around the nodes share the capacity. Therefore, we define the set of shared capacity links for each combination of node v and frequency channel c as follows.

$$S_v^c = \{(v, u, c') | (v, u, c') \in E, 0 < I_{rrr}(c, c')\} \cup \{(u, a, c) | (u, a, c) \in E, d(u, v) < R\} \quad (2)$$

In Fig. 5, $u \in V$ is a node within the *carrier-sense range* of node $v \in V$ under CCI, and $a \in V$ is within the *communication range* of u. Note that v and a may be the same node. The dotted arrow indicates that an NIC on node v is assigned with channel c. If another NIC on v is assigned with c' and link (v, u, c') exists, and c and c' are not orthogonal

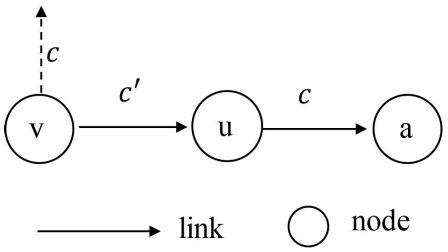

FIGURE 5. Shared link capacity model.

TABLE 3. Notations for TAC-POCA.

Symbol	Description
V	A set of nodes (routers)
E	A set of directed links
G	A directed network
Θ	Link capacity (common with all links)
N_v	The number of NICs on each node
C	A set of channels
R	Communication range of the same channel.
J	Interference range.
D	A traffic demand matrix
$D(s,d)$	A traffic demand from s to d
$l/(u,v,c)$	A link
S_{ILP}	A set of interference link pairs
S_v^c	A set of shared capacity links
R_v^c	Binary variable indicating node v is assigned with channel c or not
$P_l^{(s,d)}$	Binary variable indicating whether the path for $D(s,d)$ includes link l or not
A_l	Binary variable indicating link l is active or not
U_{max}	Real variable indicating maximum link utilization among all the links in the network.
$I_{rrr}(c_1,c_2)$	Reduce interference range ratio between transmission with channel c_1 and c_2.
$d(u,v)$	Euclidean distance between node u and v.

(i.e., $0 < I_{rrr}(c,c')$), they show the SI relationship and share the capacity Θ of S_v^c. Also, if link (u,a,c) exists, it also shares the capacity Θ of S_v^c. Here, note again that the transmission of u on channel c' is not sensed by v on channel c owing to the special treatment of POCs. Thus, if link (u,a,c') where $c \neq c'$ exists, the link is not included in S_v^c. Rather, it is treated as the collision link as in Case 3 of the CSMA-aware interference model, and a channel that does not collide with v's links is assigned to the link as a result.

The definitions in Sec III are summarized as notations in Table 3.

IV. PROBLEM FORMULATION

In this section, we formulate a joint channel assignment and routing problem in MILP based on the definition and assumptions provided in Sec III.

$$min\ U_{max} \tag{3}$$

$$Subject\ to \sum_{c\in C} R_v^c \le N_v, \quad \forall\ v \in V, \tag{4}$$

$$R_v^c \le \sum_{(v,u,c)\in E} A_{(v,u,c)} + \sum_{(u,v,c)\in E} A_{(u,v,c)},$$
$$\forall\ c \in C\ ,\ \ \forall\ v \in V, \tag{5}$$

$$A_{(u,v,c)} \le R_v^c,\ \ A_{(u,v,c)} \le R_u^c,\ \ \forall\ (u,v,c) \in E, \tag{6}$$

$$A_{l_1} + A_{l_2} \le 1, \qquad \forall\ (l_1,l_2) \in S_{ILP}, \tag{7}$$

$$\sum_{(u,v,c)\in E} P_{(u,v,c)}^{(s,d)} D(s,d) - \sum_{(v,w,c)\in E} P_{(v,w,c)}^{(s,d)} D(s,d)$$
$$= \begin{cases} -D(s,d), \text{if } v = s, \\ D(s,d), \text{if } v = d, \\ 0, \text{otherwise}, \end{cases} \quad \forall (s,d) \in V \times V, \tag{8}$$

$$\sum_{(s,d)\in V\times V} P_l^{(s,d)} \le MA_l, \quad \forall\ l \in E, \tag{9}$$

$$\sum_{(s,d)\in V\times V} P_l^{(s,d)} \ge A_l, \quad \forall\ l \in E, \tag{10}$$

$$\sum_{(s,d)\in V\times V, l\in S_v^c} D(s,d) P_l^{(s,d)}$$
$$\le U_{max}\Theta + (1 - R_v^c)W,$$
$$\forall\ v \in V, \quad \forall\ c \in C, \tag{11}$$

$$\sum_{l\in E} P_l^{(s,d)} \le \delta_{s\to d} + k, \quad \forall\ (s,d) \in V \times V, \tag{12}$$

where

$$0 \le U_{max} \le 1, \tag{13}$$

$$R_v^c \in \{0,1\}, \quad \forall\ c \in C,\ \forall\ v \in V, \tag{14}$$

$$A_l \in \{0,1\}, \quad \forall\ l \in E, \tag{15}$$

$$P_l^{(s,d)} \in \{0,1\}, \quad \forall\ (s,d) \in V \times V,\ \forall\ l \in E. \tag{16}$$

Load balancing is of utmost importance to avoid hot spots and increase network utilization. To balance the traffic in the network and prevent overloading of any link, we set (3) as the objective function to minimize the most significant link utilization in the network.

Our network topology is defined as multiple graphs in which two neighboring nodes have multiple links corresponding to each channel in C. To decrease interference, we allow the removal (i.e., inactivation) of some of the links from the topology. Therefore, the number of distinct frequency channels allocated to one node must be less than or equal to the number of NICs on each node. To represent this, we give the constraint (4).

Next, we manage the relationship among assigned channels and active links. For each node v, $(v,u,c) \in E$ denotes the output links of node v, and $(u,v,c) \in E$ denotes the input links where node u is the other terminal node of links. Then, if an NIC on node v is assigned with channel c, i.e., $R_v^c = 1$, then $\sum_{(v,u,c)\in E} A_{(v,u,c)} + \sum_{(u,v,c)\in E} A_{(u,v,c)} \ge 1$ must hold. This means that at least one connecting link (regardless of whether it is an output or input link) must be activated. This constraint is given as (5). Conversely, as indicated by (6), if none of the NICs on node v is assigned with channel c, then $A_{(u,v,c)} = 0$, i.e., link (u,v,c) must be inactive. To achieve collision-free transmission, we set (7) to ensure that the interfering links are not used for communication simultaneously. Specifically, pair of links $(l_1,l_2) \in S_{ILP}$ cannot be activated simultaneously, i.e., if $A_{l_1} = 1$, then $A_{l_2} = 0$ must stand, and vice versa.

Traffic flows in the network must meet the conservation conditions. In (8), $P^{(s,d)}_{(u,v,c)}$ and $P^{(s,d)}_{(v,w,c)}$ denote whether the route of traffic demand (s, d) goes through the input link (u, v, c) and output link (v, w, c) of v, respectively. For each traffic demand pair (s, d), we refer to s and d as the source and destination nodes of the demand, respectively. In terms of flow conservation, the total volumes of flows sent by s must be equal to that received by d. Also, the total input and output volume of flows on every intermediate node must be equal. Therefore, if node v is the source node, i.e., $v = s$, the value of (8) is equal to $-D(s, d)$. If node v is the destination node, i.e., $v = d$, the value of (8) is equal to $D(s, d)$. Otherwise, the node is an intermediate node, and the value of (8) is equal to 0. This constraint ensures that not only the traffic flow is properly routed from s to d, but also each demand is satisfied with a single explicit route. Constraint (9) means that, when at least one traffic flow goes through link l, i.e., $\sum_{(s,d)\in V\times V} P^{(s,d)}_l \geq 1$, then the link l must be activated, where M is a constant and is sufficiently large. Constraint (10) means that if there is no traffic flow through link l, the link l must be inactivated. Those two constraints (9) and (10) keep the relationship between the traffic flow and the activated links.

Recall our shared link capacity model described in Sec III-D, where the total traffic load on the links in S^c_v cannot exceed the link capacity Θ. Therefore, if channel c is assigned to node v, i.e., $R^c_v = 1$, then $\sum_{(s,d)\in V\times V, l\in S^c_v} D(s, d)P^{(s,d)}_l \leq \Theta$ must be satisfied for c and v. Otherwise, if channel c is not assigned to node v, there is no capacity constraint on these links. Constraint (11) covers both of the cases. Specifically, if $R^c_v = 1$, $(1 - R^c_v)W$ is equal to zero, and the capacity constraint is activated; otherwise, $(1 - R^c_v)W$ is equal to W, where W is a constant and is sufficiently large, meaning that the capacity constraint is inactivated. Here, we put $U_{max}\Theta$ in place of Θ to minimize the largest link utilization U_{max} as the optimization function. As $0 \leq U_{max} \leq 1$ defined in (13), inserting U_{max} does not violate the capacity constraint. Also, by minimizing U_{max} in (3), we can explore the solution for the best load balancing performance.

On the other hand, our model allows longer routing paths to enhance load balancing performance. Longer courses enable us to compute more flexible path scheduling and improve optimality in load balancing. However, very long routes will waste the capacity and increase communication delays. Thus, we enforce each of the traffic flows from s to d to use relatively short paths. Our path length constraint is (12), where $\delta_{s\to d}$ indicates the minimum hop count to reach d from s, i.e., the shortest path length from s to d in G. $k(\geq 0)$ is the path stretch in integer, then $\delta_{s\to d} + k$ in (12) means that length of every path is limited by the shortest path length plus k. The lengths of all paths are controlled by adjusting k. Constraints (13), (14), (15), and (16) define the domains of variables described previously.

With the above formulation, our problem can assign a single path for every non-zero traffic demand pair (s, d) in D using all the available channels. Both the link capacity constraint and the collision-free constraint are fulfilled, and the most significant link utilization is minimized.

V. EVALUATION

We evaluated the performance of our TAC-POCA method with two different network topologies, i.e., the grid topology and the random topology. We conducted two parts of the evaluation. In the first part, we evaluated the optimization performance using a MILP solver. In the second, we carried out a traffic simulation using an up-to-date network simulator. We describe the details in the following sections.

A. OPTIMIZATION PERFORMANCE EVALUATION

In this evaluation, we tested the optimization performance of TAC-POCA using various values of parameters such as the path stretch k, the number of NICs, and the traffic load provided. One of the critical objectives is to examine the effect of introducing POCs. Another is to determine whether TAC-POCA has better performance than TACCA. There is no joint routing and channel assignment scheme with POCs in the literature, and no scheme except for TACCA has achieved collision-free transmission with OCs in MCMR WMNs. Thus, all past schemes except TACCA are not suitable for comparison. Since TACCA reaches a collision-free schedule but only considers OCs, we can see that the performance gain of TAC-POCA compared with TACCA comes from considering POCs. Both are examined in two scenarios with grid and random topologies.

1) METHOD

We solved our MILP problem using IBM CPLEX Optimizer version 12.10 [43] executed on a computer with Intel (R) Xeon (R) CPU E5-2698 (2.20 GHz) and 256 GB memory. As typical scenarios in WMNs, we supposed two different types of network topology, i.e., grid and random layout of wireless nodes. For the grid topology, we designed a 5×5 square grid with 400 intervals in both horizontal and vertical directions. For the random topology, we located 20 nodes with random coordination in a $1,500 \times 1,500$ m square field. We assumed that each node has a communication range R of 530 m that corresponds to 20 dBm Tx power, and we take $\Delta = \varepsilon$, where ε is a tiny number. Each NIC operated IEEE 802.11g with a communication speed of 6 Mbps; thus, the link capacity Θ was also assumed as 6 Mbps. All 13 channels defined in IEEE 802.11 2.4 GHz were used for channel assignment.

Note that the number of nodes in this scenario may be relatively small compared to the network size expected in practice. However, we choose this network size in consideration of the enormous computational complexity, which requires considerable time to test a variety of parameter values. We believe that 20-25 node scenarios enable us to demonstrate all the principles and reveal the performance of our method. Additionally, it will be possible to apply

TABLE 4. Configuration in optimization evaluation.

Items	Values
Solver	IBM CPLEX Optimizer version 12.10
Number of Channels	3 for TACCA and 13 for TAC-POCA
Number of Interfaces	≥ 2 for each node
Link Capacity	6 Mbps
Communication Range	530 meters
Δ	ε (an infinitesimal number)
Network Topology	Grid and Random
Number of Nodes	25 (Gird), 20 (Random)
Traffic Demands	12 CBR flows (Grid) 10 CBR flows (Random)

our method to more extensive networks using more capable computers in parallel.

As a traffic demand, we generated flows with highly colliding traffic that covers the entire area of the field. We generated 12 bidirectional constant bit rate (CBR) flows in the grid topology. We generated 10 CBR flows with randomly selected source and destination nodes in the random topology. We show the traffic pattern of the grid topology in Figs. 6(a) and (b), and the random topology in Fig. 6(c). Note that for the grid topology, our evaluation results were obtained as the average of these two traffic patterns.

Note that the computational complexity of the TAC-POCA problem is NP-hard, and the CPLEX computation for TAC-POCA will take longer than TACCA because of its more significant number of variables in the MILP formulation. To obtain the best possible solution, we set the relative MIP gap tolerance to $1e-04$ (default value) and set the limitation of computational time of CPLEX optimization to 48 h. The entire configuration described above is summarized in Table 4.

2) RESULTS

In Table 5, we show the effect of path stretch k on the maximum network link utility U_{max}, where each traffic flow volume is equal to 500 Kbps, and each node is equipped with 2 NICs. We set $k = 0, 2, 4, 6$ for the grid topology and $k = 0, 1, 2, 3$ for the random topology. Note that, for example, $k = 3$ in the grid topology is the same as $k = 2$ because any detour path in the grid topology is the length of the corresponding shortest path plus an even number of hops. All the results are the average of five executions. We will discuss them separately in the following.

First, we focus on the grid topology. See Table 5(a). When $k = 0$, both TACCA and TAC-POCA provide no solution because of the tight constraint to finding solutions, which implies that TAC-POCA has no apparent advantage in the shortest-path case. When $k = 2$, TAC-POCA provides solutions, but TACCA cannot offer solutions, which means that POCs enable TAC-POCA to find solutions easier than TACCA when detouring paths are allowed. When $k = 4$, we see that TAC-POCA provides better solutions than TACCA, which shows that the traffic load is balanced better in TAC-POCA than in TACCA, and the efficiency of POCs decreases the link utilization. Unfortunately, when $k = 6$,

TABLE 5. The maximum network link utility U_{max} (Avg.) with path stretch k.

k	Grid	
	TACCA	TAC-POCA
0	-	-
2	-	0.5
4	0.5	0.3333
6	0.5	0.583

"-" indicates no solution be found.
(a) Grid topology

k	Random	
	TACCA	TAC-POCA
0	-	0.2916
1	-	0.3333
2	0.4583	0.3333
3	0.4583	0.3333

"-" indicates no solution be found.
(b) Random topology

TABLE 6. The value of relative MIP gap (Avg.) with path stretch k.

k	Grid	
	TACCA	TAC-POCA
0	-	-
2	-	83.3%
4	50%	100%
6	72.9%	100%

"-" indicates no solution be found.
(a) Grid topology

k	Random	
	TACCA	TAC-POCA
0	-	finished
1	-	75.0%
2	finished	100%
3	finished	100%

"-" indicates no solution be found.
(b) Random topology

TAC-POCA does not provide better solutions than TACCA within a limited time because of its sizeable computational complexity.

Next, in Table 5(b) for the random topology, we see that TACCA does not provide solutions when $k = 0$. However, TAC-POCA provides solutions for each value of k because the diversity in node distances in the random topology enables POCs to exploit more efficient spatial reuse of channels. We also see that TAC-POCA provides better solutions (i.e., lower link utility U_{max}) than TACCA, which means that the network capacity can also be improved by using POCs. Note that in both grid and random topologies, TAC-POCA with lower k sometimes provides better solutions than that with higher k. This is because the size of the problem (i.e., the number of variables in the MILP formulation) in TAC-POCA is more significant than that in TACCA, and near-optimal solutions are not always obtained within a limited time.

To see the complexity of the problems, we show the relative MIP gap values at the end of each computation in Table 6. Here, "finished" means that the calculation had finished within 48 h so that the gap value is small enough. The gap value is generally smaller in TACCA than in TAC-POCA, meaning that TAC-POCA is more complicated to solve than TACCA. Also, the gap values increase as k increases because the search space expands as k increases to allow longer routing paths. Especially in several cases, the gap keeps 100%, which means that in TAC-POCA, it is tough to find the optimal solution even though better solutions (i.e., U_{max} values) than TACCA had been found in most of the cases.

In Table 7, we show the effect of the number of NICs with the maximum network link utility U_{max}, where each traffic flow volume is equal to 500 Kbps. We set $k = 4$ for the grid topology because this is the most miniature k with which both TAC-POCA and TACCA provided reasonable solutions. Similarly, we put $k = 2$ for the random topology. Table 7 shows that the number of NICs has no noticeable effect on the performance, which means that 2 NICs are sufficient for achieving efficient spatial reuse of channels.

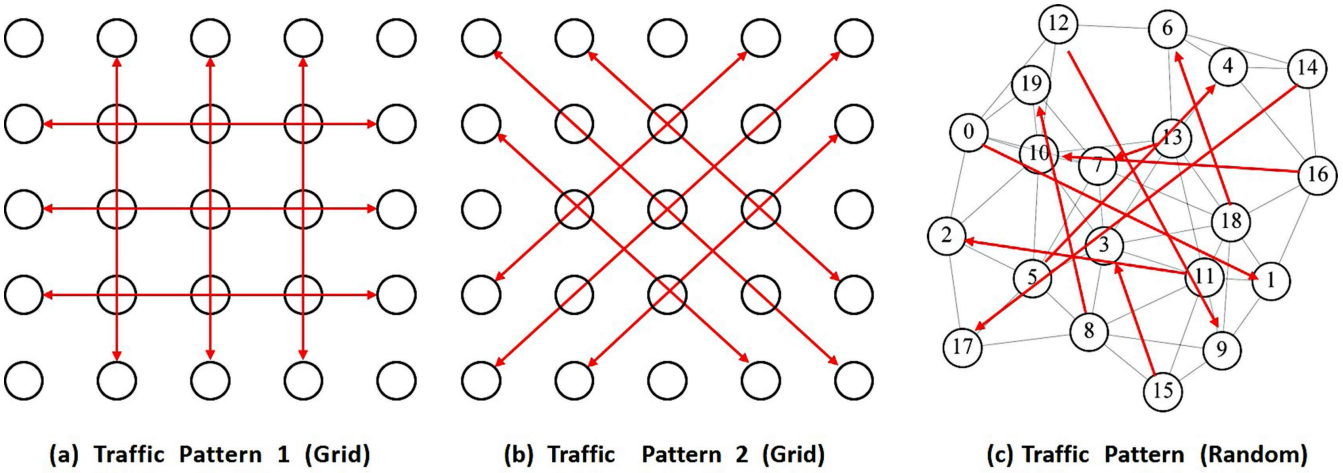

FIGURE 6. Traffic patterns.

TABLE 7. The maximum network link utility U_{max} (Avg.) with number of NICs.

NICs	Grid		Random	
	TACCA	TAC-POCA	TACCA	TAC-POCA
2	0.5	0.3333	0.4583	0.3333
3	0.5	0.3333	0.4167	0.3333
4	0.5	0.3333	0.4167	0.3333
5	0.5	0.3333	0.4167	0.2916

As shown above, in the optimization evaluation, we confirmed the property of TAC-POCA under parameter variations. TAC-POCA computes a collision-free channel assignment combined with routing configuration. Compared with TACCA, TAC-POCA efficiently uses all channels and improves the network capacity. Compared with the grid topology, which has a fixed node distance, TAC-POCA is more effective in random networks because the diversity in node distance leads to better spatial reuse of channels. On the other hand, we see that the performance of TAC-POCA has more considerable fluctuation because the complexity of the problem is more significant. TAC-POCA requires more considerable computational resources than TACCA to obtain stable results.

B. COMMUNICATION PERFORMANCE EVALUATION

1) METHOD

The simulation configuration was designed based on that of the optimization evaluation, as shown in Table 8. We equipped each node with 2 NICs that operate IEEE 802.11g at 6 Mbps speed and 20 dBm transmission power. In our preliminary experiment, 2 NICs per node were sufficient for obtaining a good schedule. Moreover, we use the IEEE 802.11g standard because it provides essential CSMA functions without additional mechanisms to increase efficiency. We chose the two-ray-ground model as the radio propagation model. The identical topologies as those in the optimization evaluation were used: a 5×5 grid topology with 400 m intervals and a $1,500 \times 1,500$ m square field random topology with 20 nodes. We generated 12 bidirectional CBR flows in the grid topology and ten flows with a random source and destination selection in the random topology. A commercial network simulator, Scenargie version 2.1 [44] was used for simulation, which implements up-to-date PHY and MAC models and adopts equivalent-level models with the commonly used network simulators ns-3 and Qualnet. Their simulation performance was verified by calibration.

We used a channel assignment and routing schedule obtained in the optimization evaluation. Specifically, we chose the schedule computed with $k = 4$ for the grid topology, $k = 2$ for the random topology, and the provides traffic load of 500 Kbps per flow. We targeted the mesh networks built with IEEE 802.11 technologies, so all the 13 channels in the 2.4 GHz band are used. Generally, the 2.4 GHz band is regarded as more valuable than the 5 GHz band for mesh infrastructure in many cases mainly because the 2.4 GHz band is more robust against obstacles than the 5 GHz band and easier to maintain wireless link connection.

We compare the performance of TAC-POCA with those of TACCA and [26], which we call Mohsenian-Rad-POCA (MR-POCA). There is no joint POC assignment and routing scheme for CSMA-based MRMC WMNs. Thus, most of the past schemes in the literature are not comparable to our scheme in terms of performance. Since TACCA achieves a collision-free schedule but uses OCs, we can see that the performance gain of TAC-POCA comes from considering POCs. Therefore, TACCA schedules with the same parameters were used in the comparison. In MR-POCA, we used the shortest path as its predetermined route. We set the appropriate parameters of the SINR-based interference model that matched our simulation parameters, such as the transmission power and IEEE 802.11 channel bandwidth.

We used the same scenarios as those for the optimization evaluation (shown in Figs.6(a) - (c)) and ran the simulator for 5000 s. We measured the average communication

performance of five repeated executions, and we compared the performance in terms of packet delivery ratio, throughput, end-to-end delivery delay, and frame drop. In this study, frame drop was included to show the network's state of collision and interference. In both scenarios, we applied flow volume variations to determine the networks' capacity.

2) RESULTS

We show the results of the grid topology in Figs. 7(a) - (d). The results are the average of the two different scenarios shown in Figs. 6(a) and (b).

In Fig. 7(a), we show the packet delivery ratio as a function of the offered traffic volume on the horizontal axis. Here, we see that both TAC-POCA and TACCA maintain an almost 100% packet delivery except where the traffic volume reaches their network capacity, meaning that the collision-freedom property in the schedule persists in the simulation. We found that the delivery rate of TACCA decreases earlier, i.e., with a lower traffic load than TAC-POCA. This is because TAC-POCA has a more efficient spatial reuse of channels, resulting in reducing the maximum link utilization. In contrast, in MR-POCA, the delivery ratio gradually decreases as traffic volume increases, even when the traffic volume is relatively low. We confirmed that this is mainly caused by the collision of RTS/CTS frames due to hidden terminal problems.

In Fig. 7(b), we show the aggregated throughput of the two schemes as a function of the offered traffic volume in the horizontal axis, where the aggregated throughput is the sum of the data rates delivered to all terminals in a network. It showed good performance when the offered load is low in both TACCA and TAC-POCA, which proves that the load balancing function worked well to increase network capacity. Owing to its high efficiency in channel utilization, TAC-POCA provided extra capacity space to support more considerable traffic, which improved the aggregate throughput. Therefore, the unexpected increase in traffic often seen in natural environments is more likely to be accommodated and can be accepted by TAC-POCA. In MR-POCA, a considerable number of packets became stuck at source nodes. This is because MR-POCA uses the shortest path routing. As a result, MR-POCA shows far lower performance than TACCA and TAC-POCA in network capacity.

We show the packet delivery delay in Fig. 7(c). We see that the delivery delay rapidly increases when the network saturates (i.e., when the traffic load exceeds the capacity of some links) in MR-POCA; this is due to the shortest path routing. In TAC-POCA and TACCA, the delay growth rate is relatively low. However, a more flexible channel assignment enables TAC-POCA to choose shorter paths, leading to a minor delay than in the case of TACCA.

Fig. 7(d) shows the status of frame loss in the MAC layer due to collision or interference. In MR-POCA, the frame loss increases as the volume of traffic increases. We see many dropped frames when the limit of retransmission count is exceeded, and most of them are due to the collision of the hidden terminal problem. In contrast, we see that the number of dropped frames is minimal in both TAC-POCA and TACCA. Through the log files, we observed only a few dropped frames; although there were several cases of interference or simultaneous backoff expiration among frames, most of them were recovered by CSMA's frame retransmission. As a result, TAC-POCA and TACCA have almost no frame loss due to interference. This implies that the interference model in TAC-POCA performed well in reducing the interference among nodes. In theory, TAC-POCA and TACCA are both collision-free transmission schemes, which achieve 100% packet delivery without collision under their interference model. On the other hand, in the simulation running with the SINR interference model, although we observed a certain level of the collision caused by interference, the collision among frames is recovered by frame retransmissions.

In Figs. 7(e) - (h), we show the same set of results in the random topology scenario. Note that the result is the average of five different random scenarios. Although the performance is slightly better than the grid scenario, the general trend is the same as the grid scenario. Namely, TAC-POCA has higher network capacity under the given traffic demand and keeps an almost 100% packet delivery with a higher offered load than TACCA and MR-POCA. Taking together, we conclude that TAC-POCA outperforms TACCA and MR-POCA in both grid and random scenarios, and it can keep the number of collisions is minimal with a higher offered load than TACCA.

3) DISCUSSION

Finally, we will discuss the value of Δ. We additionally show the evaluation results with various values of Δ in TAC-POCA. Table 9 shows the results of the optimization evaluations, which are executed with the same parameter values as are used in Sec. V-A. except that the values of Δ takes 0.0, 0.25, 0.50, 0.75, and 1.00. In both grid and random scenarios, the results show that smaller Δ achieves better optimization, which is natural because larger Δ means a larger interference range. We could not obtain any solution with $\Delta = 1.00$ in the grid and $\Delta \geq 0.75$ in the random scenario because the interference range was too large to find feasible solutions. We also show the simulation results in Fig. 8, which are obtained with the same parameter values as are used in Sec. V-B except for varying the values of Δ. Figs. 8(a)-(d) shows the results of the grid scenario, in which we see that the performance is better when Δ is smaller. We also see that the frame drop rate is always meager. This means that TAC-POCA works ideally to avoid collisions of frames with any values of Δ, and thus the optimization performance directly reflects on the communication performance. Note that the performance for $\Delta = 0.25$ and $\Delta = 0.50$ cases occur because their schedules are precisely the same; In the grid scenario, the interference ranges of both cases include the same set of nodes because of the regularity of the node locations. Figs. 8(e)-(h) shows the results of the random scenario, in which similar trends to the grid scenario are seen. The performance with smaller Δ is better because of the better

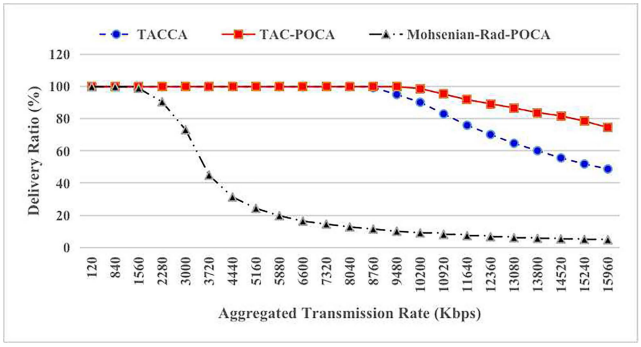

(a) Delivery Ratio (Grid Topology)

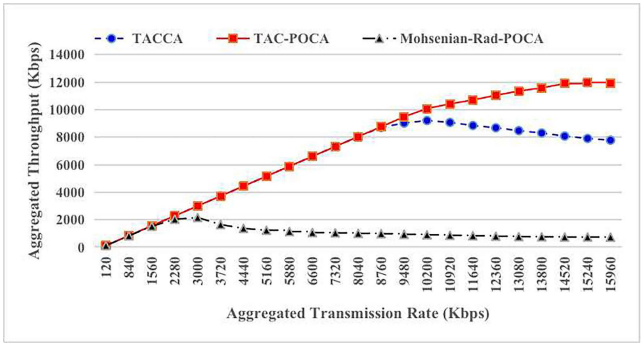

(b) Throughput (Grid Topology)

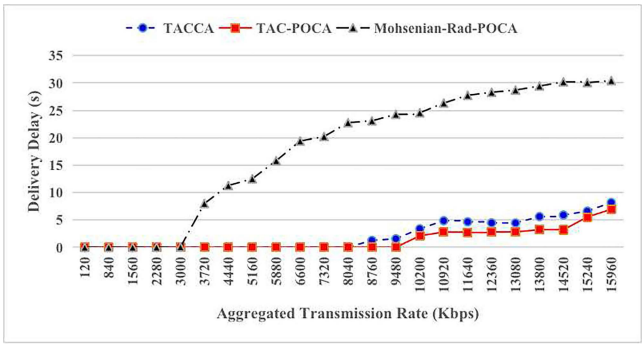

(c) Delivery Delay (Grid Topology)

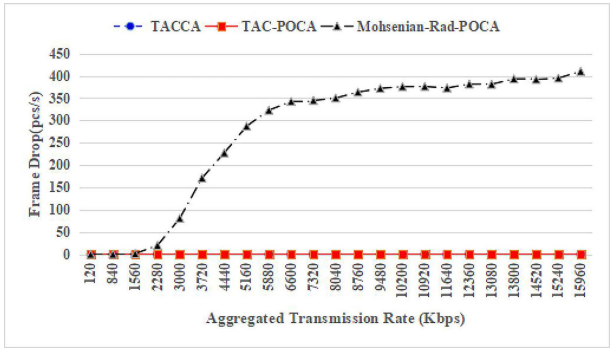

(d) Frame Drop (Grid Topology)

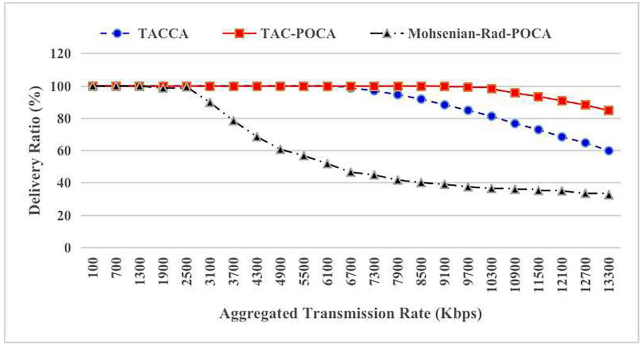

(e) Delivery Ratio (Random Topology)

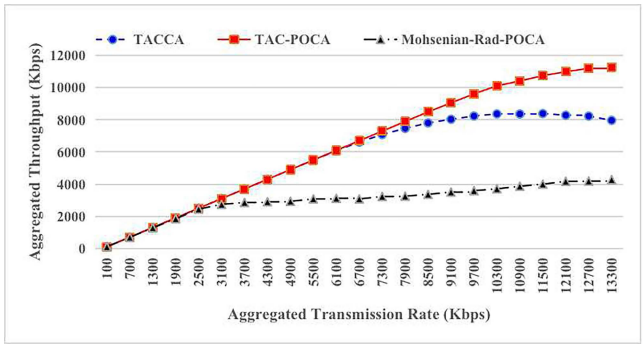

(f) Throughput (Random Topology)

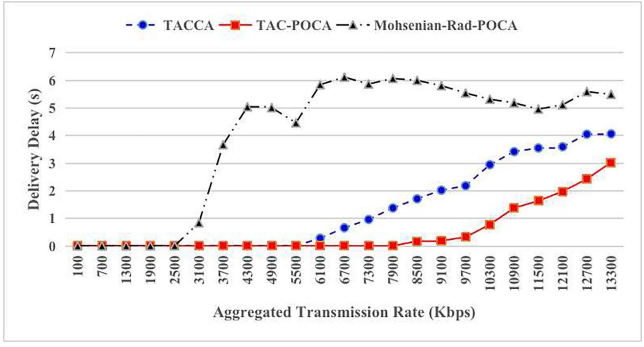

(g) Delivery Delay (Random Topology)

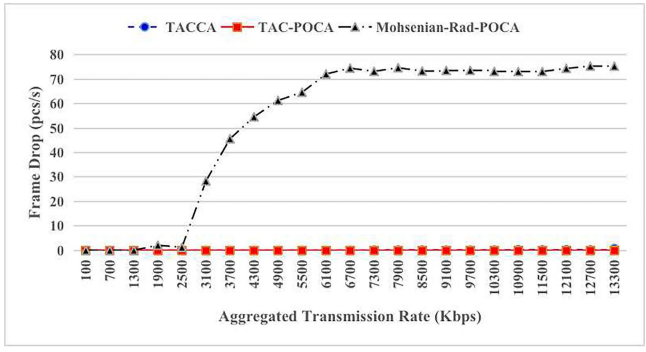

(h) Frame Drop (Random Topology)

FIGURE 7. **Communication performance evaluation.**

performance in the optimization part. In the random scenario, a slightly larger number of frame drops than in the grid scenario were observed, as shown in Fig. 8(h), but it was tiny and negligible. We confirmed that the smaller Δ performs better in grid and random scenarios and the low frame drop rate. Since we had an excellent result on frame drops, we can conclude that the value $\Delta = \varepsilon$ is the best in our scenarios with TAC-POCA.

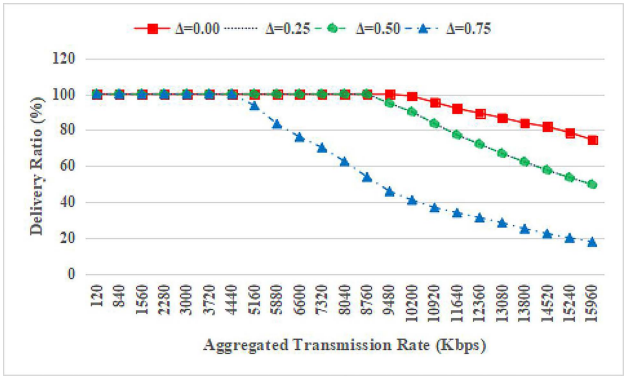

(a) Delivery Ratio (Grid Topology)

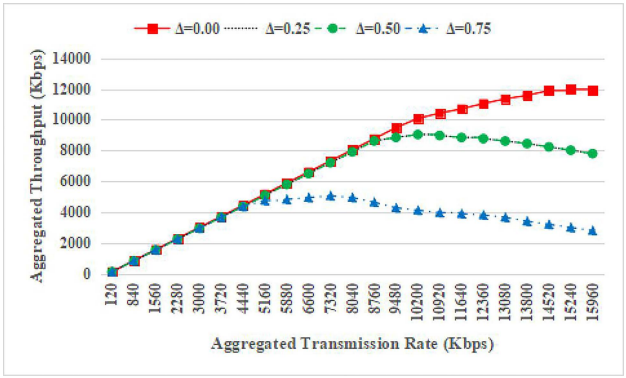

(b) Throughput (Grid Topology)

(c) Delivery Delay (Grid Topology)

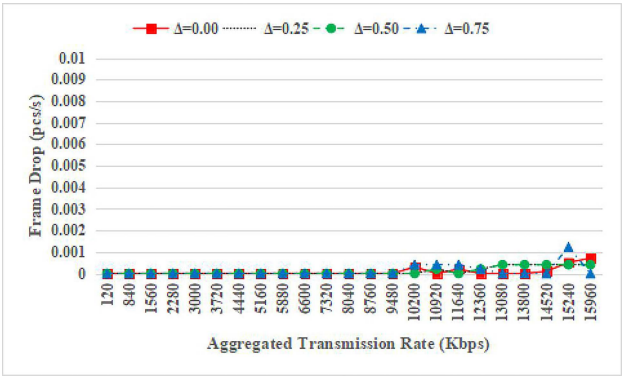

(d) Frame Drop (Grid Topology)

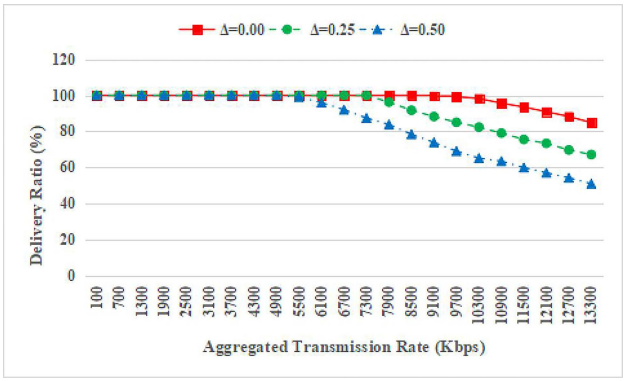

(e) Delivery Ratio (Random Topology)

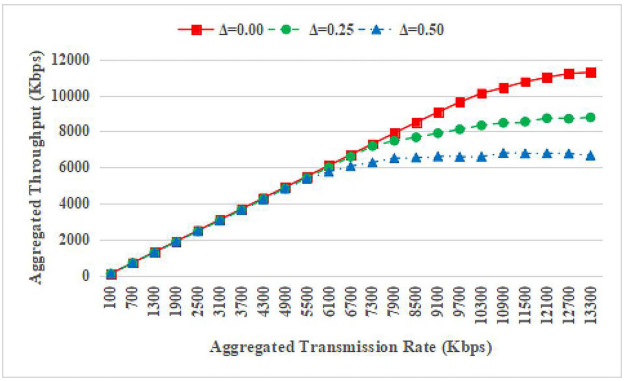

(f) Throughput (Random Topology)

(g) Delivery Delay (Random Topology)

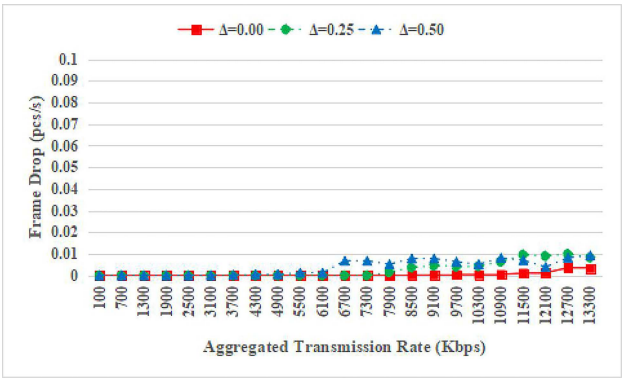

(h) Frame Drop (Random Topology)

FIGURE 8. **Communication performance evaluation of different interference range.**

TABLE 8. Configuration in traffic simulation.

Items	Values
Simulator	Scenargie version 2.1
PHY and MAC Protocols	IEEE802.11g
Propagation Model	Two ray ground
Link Capacity	6 Mbps
Transmission Power	20 dBm
Number of Interfaces	2 for each node
Number of Channels	3 for TACCA and 13 for TAC-POCA
Communication Range	530 m
Network Topology	Grid and Random
Traffic Demands	12 CBR flows (Grid) 10 CBR flows (Random)
Payload Size	1472 bytes
Number of Nodes	25 (Grid) and 20 (Random)
Simulation Time	5000 seconds

TABLE 9. The maximum network link utility U_{max} (Avg.) with the value of Δ.

Δ	Grid	Random
0.25	0.667	0.500
0.50	0.667	0.625
0.75	0.833	-
1.00	-	-

"-" indicates no solution be found.

VI. CONCLUSION

By exploiting all the channels defined in IEEE 802.11 2.4 GHz band channels, we designed a new joint channel assignment and routing scheme using POC interference models. The proposed scheme called TAC-POCA significantly improved the spatial reuse of radios. It achieved collision freedom combined with the CSMA-aware interference model and the shared link capacity model extended for POCs. Although TACCA has already attained a collision-free channel assignment and routing using OCs, TAC-POCA significantly improved the spatial reuse of radios and network capacity by applying POCs.

We conducted two evaluations, i.e., optimization and simulation evaluations, and showed that POCs significantly improve the spatial reuse in joint channel assignment and routing. In particular, we found that the variations of distance in the random layout exploit the ability of POCs. Furthermore, we confirmed that TAC-POCA keeps a very low level of collision even in-network simulations with the SINR-based interference model. The proposed CSMA-aware interference model with POCs works in networks.

As a limitation, due to many variables in MILP formulation, TAC-POCA requires more considerable computational resources to achieve stable output results. Since the channel assignment problem is NP-hard, designing a good heuristic algorithm will be a future task. Introducing the SINR-based interference model to the joint routing and channel assignment schemes will be another enjoyable future task.

REFERENCES

[1] I. F. Akyildiz and X. Wang, *Wireless Mesh Networks*. Hoboken, NJ, USA: Wiley, 2009, pp. 1–13.

[2] J. R. Parvin, "An overview of wireless mesh networks," in *Wireless Mesh Networks-Security, Architectures and Protocols*. Rijeka, Croatia: IntechOpen, Jun. 2019. [Online]. Available: https://www.intechopen.com/online-first/an-overview

[3] W. Tu, "Efficient wireless multimedia multicast in multi-rate multi-channel mesh networks," *IEEE Trans. Signal Inf. Process. Over Netw.*, vol. 2, no. 3, pp. 376–390, Sep. 2016.

[4] G. S. L. K. Chand, M. Lee, and S. Y. Shin, "Drone based wireless mesh network for disaster/military environment," *J. Comput. Commun.*, vol. 6, no. 4, p. 44, 2018.

[5] D. J. David, V. Jegathesan, T. J. Jebaseeli, and A. B. Ambrose, "Recent trends in channel assignment techniques in wireless mesh networks," in *Deep Learning Strategies for Security Enhancement in Wireless Sensor Networks*. Hershey, PA, USA: IGI Global, 2020, pp. 155–176.

[6] H. A. Mogaibel, M. Othman, S. Subramaniam, and N. A. W. A. Hamid, "Review of channel assignment approaches in multi-radio multi-channel wireless mesh network," *J. Netw. Comput. Appl.*, vol. 72, pp. 113–139, Sep. 2016.

[7] A. Raniwala, K. Gopalan, and T. C. Chiueh, "Centralized channel assignment and routing algorithms for multi-channel wireless mesh networks," *ACM SIGMOBILE Mobile Comput. Commun. Rev.*, vol. 8, no. 2, pp. 50–65, 2004.

[8] O. M. Zakaria, A. H. A. Hashim, W. H. Hassan, O. O. Khalifa, M. Azram, L. B. Jivanadham, M. L. Sanni, and M. Zareei, "Joint channel assignment and routing in multiradio multichannel wireless mesh networks: Design considerations and approaches," *J. Comput. Netw. Commun.*, vol. 2016, Jun. 2016, Art. no. 2769685.

[9] Y. Qu, B. Ng, and W. Seah, "A survey of routing and channel assignment in multi-channel multi-radio WMNs," *J. Netw. Comput. Appl.*, vol. 65, pp. 120–130, Apr. 2016.

[10] A. B. M. Alim Al Islam, M. J. Islam, N. Nurain, and V. Raghunathan, "Channel assignment techniques for multi-radio wireless mesh networks: A survey," *IEEE Commun. Surveys Tuts.*, vol. 18, no. 3, pp. 988–1017, 2nd Quart., 2016.

[11] A. Musaddiq, F. Hashim, C. A. B. C. Ujang, and B. M. Ali, "Survey of channel assignment algorithms for multi-radio multi-channel wireless mesh networks," *IETE Tech. Rev.*, vol. 32, no. 3, pp. 164–182, May 2015.

[12] A. Mishra, E. Rozner, S. Banerjee, and W. Arbaugh, "Exploiting partially overlapping channels in wireless networks: Turning a peril into an advantage," in *Proc. 5th ACM SIGCOMM Conf. Internet Meas.*, 2005, p. 29.

[13] A. Mishra, V. Shrivastava, S. Banerjee, and W. Arbaugh, "Partially overlapped channels not considered harmful," in *Proc. Joint Int. Conf. Meas. Model. Comput. Syst. (SIGMETRICS /Performance)*, 2006, pp. 63–74.

[14] F. Bokhari and G. Zaruba, *Partially Overlapping Channel Assignment in Wireless Mesh Networks*. Aug. 2012, doi: 10.5772/48476.

[15] X. Zhao, L. Li, S. Geng, H. Zhang, and Y. Ma, "A link-based variable probability learning approach for partially overlapping channels assignment on multi-radio multi-channel wireless mesh information-centric IoT networks," *IEEE Access*, vol. 7, pp. 45137–45145, 2019.

[16] J. Wang, W. Shi, K. Cui, F. Jin, and Y. Li, "Partially overlapped channel assignment for multi-channel multi-radio wireless mesh networks," *EURASIP J. Wireless Commun. Netw.*, vol. 2015, no. 1, p. 25, Dec. 2015.

[17] P. B. F. Duarte, Z. M. Fadlullah, A. V. Vasilakos, and N. Kato, "On the partially overlapped channel assignment on wireless mesh network backbone: A game theoretic approach," *IEEE J. Sel. Areas Commun.*, vol. 30, no. 1, pp. 119–127, Jan. 2012.

[18] M. A. Hoque and X. H. F. Afroz, "Multiple radio channel assignement utilizing partially overlapped channels," in *Proc. IEEE Global Telecommun. Conf. (GLOBECOM)*, Nov./Dec. 2009, pp. 1–7.

[19] K. Liu, N. Li, and Y. Liu, "Min-interference and connectivity-oriented partially overlapped channel assignment for multi-radio multi-channel wireless mesh networks," in *Proc. 3rd IEEE Int. Conf. Comput. Commun. (ICCC)*, Dec. 2017, pp. 84–88.

[20] F. S. Bokhari and G. V. Zaruba, "I-POCA: Interference-aware partially overlapping channel assignment in 802.11-based meshes," in *Proc. IEEE 14th Int. Symp. 'World Wireless, Mobile Multimedia Netw.' (WoWMoM)*, Jun. 2013, pp. 1–6.

[21] Y. Ding, Y. Huang, G. Zeng, and L. Xiao, "Using partially overlapping channels to improve throughput in wireless mesh networks," *IEEE Trans. Mobile Comput.*, vol. 11, no. 11, pp. 1720–1733, Nov. 2012.

[22] Y. Tian, T. Noi, and T. Yoshihiro, "Achieving hidden-terminal-free channel assignment in IEEE802.11-based multi-radio multi-channel wireless mesh networks," *IEICE Trans. Commun.*, vol. 104, no. 7, pp. 873–883, 2021.

[23] L. Yang, Y. Li, S. Wang, and H. Xiao, "Interference-avoid channel assignment for multi-radio multi-channel wireless mesh networks with hybrid traffic," *IEEE Access*, vol. 7, pp. 67167–67177, 2019.

[24] J. Wang and W. Shi, "Partially overlapped channels- and flow-based end-to-end channel assignment for multi-radio multi-channel wireless mesh networks," *China Commun.*, vol. 13, no. 4, pp. 1–13, 2016.
[25] Y. Liu, R. Venkatesan, and C. Li, "Load-aware channel assignment exploiting partially overlapping channels for wireless mesh networks," in *Proc. IEEE Global Telecommun. Conf. (GLOBECOM)*, Dec. 2010, pp. 1–5.
[26] A. H. M. Rad and V. W. S. Wong, "Partially overlapped channel assignment for multi-channel wireless mesh networks," in *Proc. IEEE Int. Conf. Commun.*, Jun. 2007, pp. 3770–3775.
[27] Y. Tian and T. Yoshihiro, "Traffic-demand-aware collision-free channel assignment for multi-channel multi-radio wireless mesh networks," *IEEE Access*, vol. 8, pp. 120712–120723, 2020.
[28] Y. Tian and T. Yoshihiro, "Collision-free channel assignment with overlapped channels in multi-radio multi-channel wireless mesh networks," in *Proc. Int. Conf. Mobile Ubiquitous Syst., Comput., Netw., Services*. Cham, Switzerland: Springer, 2021, pp. 681–692.
[29] J. Liu, W. Shi, and P. Wu, "Joint routing and channel assignment in multi-rate wireless mesh networks," *KSII Trans. Internet Inf. Syst.*, vol. 11, no. 5, pp. 2362–2378, 2017.
[30] P. Cappanera, L. Lenzini, A. Lori, G. Stea, and G. Vaglini, "Optimal joint routing and link scheduling for real-time traffic in TDMA wireless mesh networks," *Comput. Netw.*, vol. 57, no. 11, pp. 2301–2312, Aug. 2013.
[31] M. Alicherry, R. Bhatia, and L. Li, "Joint channel assignment and routing for throughput optimization in multi-radio wireless mesh networks," in *Proc. 11th Annu. Int. Conf. Mobile Comput. Netw. (MobiCom)*, 2005, pp. 58–72.
[32] A. U. Chaudhry, R. H. M. Hafez, and J. W. Chinneck, "On the impact of interference models on channel assignment in multi-radio multi-channel wireless mesh networks," *Ad Hoc Netw.*, vol. 27, pp. 68–80, Apr. 2015.
[33] A. U. Chaudhry, J. W. Chinneck, and R. H. M. Hafez, "Fast heuristics for the frequency channel assignment problem in multi-hop wireless networks," *Eur. J. Oper. Res.*, vol. 251, no. 3, pp. 771–782, Jun. 2016.
[34] A. U. Chaudhry, R. H. M. Hafez, and J. W. Chinneck, "Realistic interference-free channel assignment for dynamic wireless mesh networks using beamforming," *Ad Hoc Netw.*, vol. 51, pp. 21–35, Nov. 2016.
[35] M. Islam, M. A. Razzaque, and M. Mamun-Or-Rashid, "Joint link-channel selection and power allocation in multi-radio wireless mesh networks," in *Proc. IEEE 18th Int. Symp. A World Wireless, Mobile Multimedia Netw. (WoWMoM)*, Jun. 2017, pp. 1–7.
[36] S. Avallone, F. P. D'Elia, and G. Ventre, "A new channel, power and rate assignment algorithm for multi-radio wireless mesh networks," *Telecommun. Syst.*, vol. 51, no. 1, pp. 73–80, Sep. 2012.
[37] J. Jia, X. Wang, and J. Chen, "A genetic approach on cross-layer optimization for cognitive radio wireless mesh network under SINR model," *Ad Hoc Netw.*, vol. 27, pp. 57–67, Apr. 2015.
[38] H. Cheng and S. Yang, "Joint QoS multicast routing and channel assignment in multiradio multichannel wireless mesh networks using intelligent computational methods," *Appl. Soft Comput.*, vol. 11, no. 2, pp. 1953–1964, Mar. 2011.
[39] K. Gokbayrak and E. A. Yildirim, "Joint gateway selection, transmission slot assignment, routing and power control for wireless mesh networks," *Comput. Oper. Res.*, vol. 40, no. 7, pp. 1671–1679, Jul. 2013.
[40] K. Zhou, H. Yuan, Z. Zhang, X. Ao, and H. Zhao, "Joint topology control and channel assignment employing partially overlapping channels in multirate wireless mesh backbone," *Int. J. Wireless Inf. Netw.*, vol. 25, no. 2, pp. 209–220, Jun. 2018.
[41] W. Hassan and T. Farag, "Adaptive allocation algorithm for multi-radio multi-channel wireless mesh networks," *Future Internet*, vol. 12, no. 8, p. 127, Jul. 2020.
[42] P. Gupta and P. R. Kumar, "The capacity of wireless networks," *IEEE Trans. Inf. Theory*, vol. 46, no. 2, pp. 388–404, Mar. 2000.
[43] *IBM CPLEX Optimizer*. Accessed: Feb. 10, 2020. [Online]. Available: https://www.ibm.com/analytics/cplex-optimizer
[44] *Scenargie VisualLab & Base Simulator—SPACE-TIME*. Accessed: Aug. 1, 2020. [Online]. Available: https://www.spacetime-eng.com/en/

YI TIAN (Graduate Student Member, IEEE) received the B.S. degree from the Kunming University of Science and Technology, Kunming, China, in 2005, the M.S. degree from Northwest University, Xi'an, China, in 2011, and the Ph.D. degree from Wakayama University, Wakayama, Japan, in 2021. He has been an Associate Professor with Shangluo University, since 2016. His research interests include computer networks and wireless networks.

TAKUYA YOSHIHIRO (Member, IEEE) received the B.E., M.I., and Ph.D. degrees from Kyoto University, in 1998, 2000, and 2003, respectively. He was an Assistant Professor at Wakayama University, from 2003 to 2009, where he has been an Associate Professor, since 2009. He is currently interested in graph theory, distributed algorithms, computer networks, wireless networks, medical applications, bioinformatics, IoT, and data ecosystems. He is a member of ACM, IEICE, and IPSJ.